The Compact Manifold of Stellar Objects Spinning Around the Supermassive Black Hole in the Galactic Center: The Laboratory of Projective Symplectic Orbiton/Spinon Dynamics

Walter Schempp
Lehrstuhl fuer Mathematik I, University of Siegen
D 57068 Siegen, Germany
schempp@mathematik.uni-siegen.de

Abstract
Based on projective differential geometry, a quantum holographic approach to the post–Keppleriam orbiton/spinon dynamics of quantum blackholography and clinical magnetic resonance tomography is mathematically described. Crucial applications of the conformal steady–state free–precession modality and automorphic scattering theory are the compelling evidence for a supermassive central black hole in the Milky Way galaxy.
Keywords : Blackholography, mathematical radiology, quantum field theory, harmonic analysis of the real Heisenberg Lie group, quantum entangled symplectic spinors, Hopf fibration and tangential Hopf link, Kerr's exact solution of the Einstein vacuum field equations

Et habet ipsa etiam prolixitas phrasium suam obscuritatem, non minorem quam concisa brevitas (Johannes Keppler, 1571–1630).

1 Introductory Overview

The concept of balanced steady–state free–precession, well known from the synchronization procedure of cardiac magnetic resonance tomography, can be traced back to the epoch–making treatise *Astronomia Nova* published by Johannes Keppler in 1609. In view of the fact that the universe is basically a quantum physical construction, the orbiton/spinon dynamics of the Keppler space observatory, launched by NASA on March 5th, 2009 on a earth–trailing heliocentric trajectory to discover earth–sized and smaller *extrasolar* planets or exoplanets of the Milky Way galaxy in or near the habitable zone, tries to determine how many of the billions of stars in the Galaxis have such stars.

A terrestric analog of the Keppler space telescope with the earth as host star is the orbiton/spinon controlled *Nightpod* technology of the International Space Station ISS. The *Nightpod* optical instrument is positioned in the observation cupola of the spacecraft on its geocentric trajectory. It represents an interesting application

International Journal of Computing Anticipatory Systems, Volume 27, 2014
Edited by D. M. Dubois, CHAOS, Liège, Belgium, ISSN 1373-5411 ISBN 2-930396-16-4

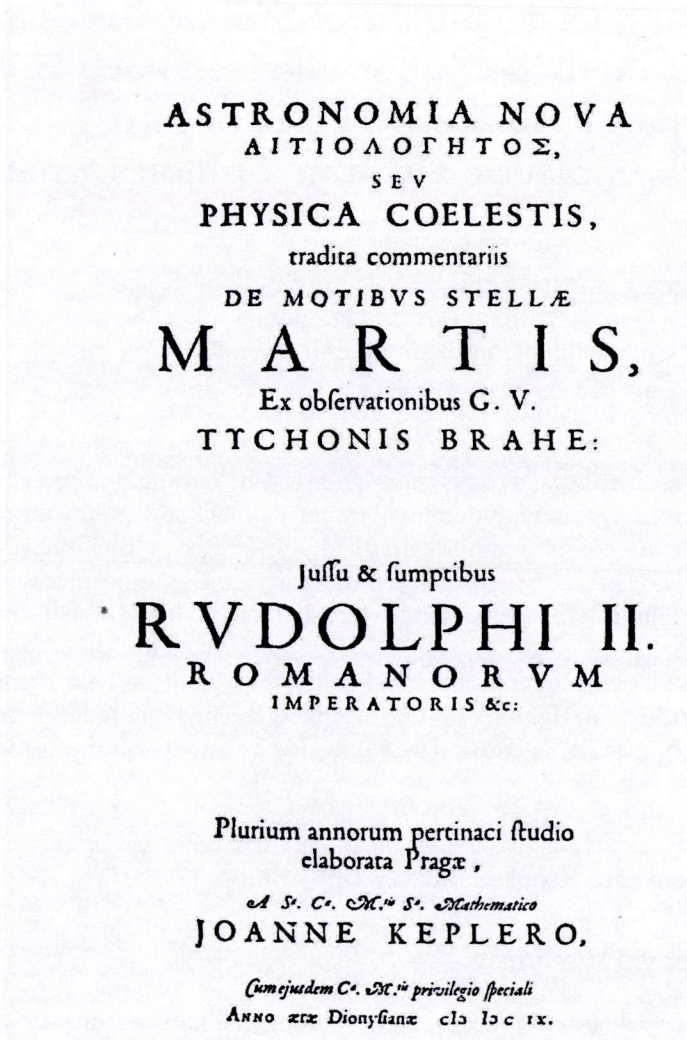
ASTRONOMIA NOVA
AITIOΛOΓHTOΣ,
SEV
PHYSICA COELESTIS,
tradita commentariis
DE MOTIBVS STELLÆ
MARTIS,
Ex obſervationibus G. V.
TYCHONIS BRAHE:

Juſſu & ſumptibus
RVDOLPHI II.
ROMANORVM
IMPERATORIS &c:

Plurium annorum pertinaci ſtudio
elaborata Pragæ,

A S^r. C^a. M.^te S^r. Mathematico
JOANNE KEPLERO,

Cum ejusdem C^a. M.^te privilegio ſpeciali
ANNO æræ Dionyſianæ CIↃ IↃC IX.

Fig. 1: Title page of Johannes Keppler's treatise *Astronomia Nova* of 1609 indicating the role of the planet Mars for the Kepplerian astrophysical studies. For the first time they are concerned with a mathematical treatment of the orbiton/spinon dynamics of balanced steady–state free–precession. Based on Tycho Brahe's long–term observations with unaided eyes, the first and second Kepplerian law of planetary motion have been established and conformally visualized in the record of a decade's intense labor.

of the orbiton/spinon dynamics of balanced steady–state free–precession, which is implemented by the seesaw pair configuration displayed infra.

The seesaw pair detachment diagram establishes the planetary laws of the Keplerian projective libration theory of harmonic oscillations (*libra* = torsion balance, already known to Copernicus) by acting in the three–dimensional real projective space $\mathbb{P}_3(\mathbb{R})$ of spin–tags

$$\begin{array}{cc} \mathrm{O}(\mathbb{C}_{\mathbb{R}} \oplus \bar{\mathbb{C}}_{\mathbb{R}}, \mathbb{R}) & \mathrm{Sp}(2,\mathbb{R}) \times \mathrm{Sp}(2,\mathbb{R}) \\ & \bowtie \\ \mathrm{O}(2,\mathbb{R}) \times \mathrm{O}(2,\mathbb{R}) & \mathrm{Mp}(2,\mathbb{R}), \end{array}$$

In the seesaw pair diagram, the vertical arrows visualize embeddings and slanted arrows indicate connections of detached members of mutually *centralizing* dual reductive pairs in the spirit of orbiton/spinon dynamics, performed by the Fourier filter–bank of the unitarily exponentiated reducible metaplectic representation of $\mathrm{Mp}(2,\mathbb{R})$. The Lie group $\mathrm{Mp}(2,\mathbb{R})$ forms a two–sheeted covering group of the symplectic group $\mathrm{Sp}(2,\mathbb{R}) \cong \mathrm{SL}(2,\mathbb{R})$.

The action of the seesaw pair detachment diagram is fully consistent with the axially symmetric Kerr–Newman contact geometry for the exterior field of a stationary black hole. It forms the general solution of the Einstein field equation for a rotating, charged mass in vacuo. In the limit this geometry corresponds to an astrophysical black hole ([9], [16], [17]). To an outside observer it takes infinite time for light to reach the event horizon, and hence no radiation is detected from a black hole. Due to the *conformality* of the Möbius inversion in a sphere, it extends projectively the stationary, spherically symmetric geometry of Schwarzschild space–time metric. In this context, spherical symmetry is meant that the Schwarzschild space–time is foliated by a family of geodesically parallel two–dimensional spheres, with no direction within the sphere bundle preferred.

The Schwarzschild space–time metric reads in terms of the radial tensor coordinates

$$(1, \frac{x}{r}, \frac{y}{r}, \frac{z}{r})$$

with scale factor

$$\lambda = \frac{2\, m_0}{r}$$

of geometric mass m_0 and radius $r > 0$. The space–time metric discovered by Roy Patrick Kerr in 1963, some 48 years after the Einstein vacuum field equations were first developed, forms the *only* solution of Einstein's equation among the stationary ones which is non–singular outside the horizon ([46]).

The mathematical background of his innovative space–time concept describes Kerr in the following manner:

In 1958 *I became interested in the new methods that were entering general relativity from differential geometry at that time, and the use of projective geometry.*

Neither the fiber bundle approach to projective differential geometry nor the ray–traced visualization technique of general relativity theory were available at that time. To quote Stephen William Hawking, the result of Kerr's efforts reads as follows:

The Kerr solutions are the only known family of exact solutions which could represent the stationary axisymmetric asymptotically flat field outside a rotating massive object. The Kerr solutions do appear to be the only possible exterior solutions for black holes.

In the case of the Kerr solution, the flat Minkowski space–time extends the singular plane $\nu = 0$ of the affine coadjoint orbit model $\mathrm{Lie}(\mathcal{N})^*/\mathrm{CoAd}(\mathcal{N})$ of the real Heisenberg Lie group $\mathcal{N}$. In view of the gradient controlled coordinatization technique of conformal projective differential geometry, the metaplectic spinor coordinates of the bicylindrical bore part of the axially symmetric Kerr space–time metric arising from a steadily spinning source read

$$(1, \frac{rx + \nu y}{\nu^2 + r^2}, \frac{-\nu x + ry}{\nu^2 + r^2}, \frac{z}{r}) \qquad (\nu \neq 0)$$

with scale factor

$$\lambda = \frac{2\, m_0\, r^3}{r^4 + \nu^2\, z^2}.$$

The Kerr space–time metric can be expressed in terms of the advanced Eddington–Finkelstein as well as the classical Boyer–Lindquist charts ([17]). Due to Joseph Liouville's remarkable classification of conformal mappings in terms of Möbius transformations, that is mappings that are generated by similarities and Möbius inversions in spheres, the quantum field theoretic extension of the Kepplerian planetary astrophysics reads as follows:

Theorem 1. *The quantum holographic approach to the blackholography of relativistic cosmology provides exactly two asymptotically flat stationary solutions of the* Einstein *vacuum field equations, namely*
(i) *the spherically symmetric* Schwarzschild *solution,*
(ii) *the axially symmetric* Kerr *solution.*

The preceding theorem is based on the Stone–von Neumann theorem of quantum field theory, and Liouville's infinitesimal characterization of conformal mappings of the affine coadjoint orbit model $\mathrm{Lie}(\mathcal{N})^*/\mathrm{CoAd}(\mathcal{N})$. The proof of the latter which depends upon the classical idea of a triply orthogonal family of smooth surfaces and the theorem of Pierre Charles François Dupin on umbilical intersection points of lines of curvature ([4]) does only indirectly refer to the Penrose twistor calculus ([29], [46]) with coordinates

$$\frac{i}{\sqrt{2}} \begin{pmatrix} z - t & w \\ \bar{w} & z + t \end{pmatrix} \qquad (w = x + iy \in \mathbb{C}_{\mathbb{R}})$$

of the complex Minkowski time–space. It became clear that Kerr's discovery of an exact stationary vacuum solution of the Einstein field equation that corresponds to the axially symmetric field around a steadily spinning source became the basis of black hole research. Specifically it became clear that a spinning black hole represents the unique final equilibrium configuration of any electrically neutral collapsing body.

Another highly interesting application of the orbiton/spinon dynamics of balanced steady–state free–precession which is implemented by the Fourier filter–bank of the seesaw pair detachment configuration is the general relativistic test for the existence of gravitational wave radiation by means of the rapid orbital period decay in the recently discovered detached binary white dwarf system J065133+284423. Similarly to the relativistic binary pulsar PSR B1913+16, it is based on the loss of angular momentum of the detached binary dwarf system of extreme low masses $0.26\,\mathrm{M}_\odot$ and $0.50\,\mathrm{M}_\odot$ which has been observed at optical wavelengths at a distance of about 3×10^3 light years from the earth with a 12.75 minute orbital period and a 1315 $\mathrm{km\,s^{-1}}$ radial velocity amplitude ([5], [40]).

Radio pulsars are rapidly rotating highly magnetised neutron stars. After six years of high precision observations, the astrophysicist Joseph Hooton Taylor Jr. who discovered with Russell Alan Hulse at Arecibo Observatory in 1974 the 7 hours 45 minutes relativistic binary pulsar PSR B1913+16, formulates the post–Kepplerian orbiton/spinon dynamics as follows:

Spin precession provides an unprecedented opportunity to map the radio pulsar beam in the latitude direction and a chance to observe for the first time a "magnetic" aspect of gravity.

In this way, Taylor supports Keppler's magnetic approach to spherical gravity which is based on William Gilbert's treatise *Tractatus, sive physiologia nova de magnete, magneticisque corporibus et de magno magnete tellure. Sex libris comprehensus* of 1600 ([38]).

Among the best known results of the post–Kepplerian orbiton/spinon dynamics are measurements of the relativistic advance of *perenigricon* at a rate some 35.000 times that of Mercury ([7], [41], [45]); see Figure 6. The concept of perenigricon corresponds to the perihel in the heliocentric planetary system. It is this cosmological effect which suggests a contact geometrical visualization of the stationary trajectories and their linearized focal phase shifts at perenigricon.

The importance of the seesaw pair configuration derives from the fact that it implies in terms of the Euclidean distributional Laplace operator $\Delta : \mathcal{S}'(\mathbb{R} \oplus \mathbb{R}) \longrightarrow \mathcal{S}'(\mathbb{R} \oplus \mathbb{R})$ the partial differential equation of second order

$$\frac{\partial^2 u}{\partial t^2} = y^2 \Delta u + \frac{1}{4} u \qquad (y = \Im w)$$

for the automorphic wave function $(t, w) \rightsquigarrow u(t, w)$ on the product space $\mathbb{R} \times \mathbb{C}_{\mathbb{R}}$. As a consequence of automorphic scattering theory ([22], [15]), the Schrödinger wave

equation of quantum mechanics

$$i\,\frac{\partial\psi}{\partial t} = \frac{1}{2}\,\Delta\psi$$

in standard notation arises.

The metaplectic group $\mathrm{Mp}(2,\mathbb{R})$, which admits as a double covering of the symplectic group $\mathrm{Sp}(2,\mathbb{R})$ the exact sequence

$$\{1\} \longrightarrow \mathbb{Z}_2 \longrightarrow \mathrm{Mp}(2,\mathbb{R}) \longrightarrow \mathrm{Sp}(2,\mathbb{R}) \longrightarrow \{1\}\,,$$

was first introduced in order to reformulate Carl Ludwig Siegel's analytic theory of quadratic forms in terms of group theory ([44]). As a projective representation of the symplectic group $\mathrm{Sp}(2,\mathbb{R}) \cong \mathrm{SL}(2,\mathbb{R})$, the metaplectic representation forms a genuine unitary linear group representation of $\mathrm{Mp}(2,\mathbb{R})$ which forms the basis of the projective differential geometry of symplectic spinors ([20], [21]).

In the context of the seesaw pair configuration, the involutive automorphism of the Argand plane $\mathbb{C}_{\mathbb{R}} \cong \mathbb{R}(i) \cong \mathbb{C}$, defined by the complex conjugation mapping, provides the orientation reversing spin echo transition $\mathbb{C}_{\mathbb{R}} \longrightarrow \bar{\mathbb{C}}_{\mathbb{R}}$. It forms an efficient tool of magnetic resonance spectroscopy and clinical magnetic resonance tomography ([31]). Due to the isomorphy of the Galois cohomology group

$$\mathcal{H}^2(\mathrm{Sp}(\mathbb{C}_{\mathbb{R}},\mathbb{R}),\mathbb{Z}_2) \cong \mathbb{Z}_2\,,$$

the symplectic group $\mathrm{Sp}(\mathbb{C}_{\mathbb{R}},\mathbb{R}) \cong \mathrm{Sp}(2,\mathbb{R})$ admits, up to isomorphy, a unique non–trivial extension by $\mathbb{Z}_2 = \mathbb{Z}/2\mathbb{Z}$, the metaplectic group $\mathrm{Mp}(\mathbb{C}_{\mathbb{R}},\mathbb{R}) \cong \mathrm{Mp}(2,\mathbb{R})$ which can be explicitly constructed in the exact sequence

$$\{1\} \longrightarrow \mathbb{Z}_2 \longrightarrow \mathrm{Mp}(\mathbb{C}_{\mathbb{R}},\mathbb{R}) \longrightarrow \mathrm{Sp}(\mathbb{C}_{\mathbb{R}},\mathbb{R}) \longrightarrow \{1\}$$

in terms of the Maslov index ([14]).

The phase shift due to the Maslov index provides the corrected Feynman path integral representation on phase space. Since Richard Feynman's original formula is valid only for short times, the connection of the Maslov index to the metaplectic group $\mathrm{Mp}(2,\mathbb{R})$ justifies the mathematician's care, of which Feynman emphatically complains.

The physicist cannot understand the mathematician's care in solving an idealized physical problem. The physicist knows the real problem is much more complicated. It has already been simplified by intuition which discards the unimportant and often approximates the remainder.

The orbiton/spinon dynamical subtleties hindering a thorough understanding of the modality of magnetic resonance tomography were the reason for the difficulties with its clinical reception. It was Erwin Louis Hahn who decisively changed the practical applicability of magnetic resonance tomography by the seminal discovery of the concept of *spin echo* in 1949. In pulsed nuclear magnetic resonance spectroscopy,

relaxation times are measured directly and accurately from the spin echo amplitudes. Concerning magnetic resonance tomography, Hahn wrote:

I apologize to magnetic resonance imaging (MRI) *pioneers because I never believed* MRI *would work, like* Rutherford, *who said that anyone who believed nuclear radioactivity would be useful "is talking moonshine". However, I was only one of many unbelievers. Another unfidel in particular was* Anatole Abragam, *a distinguished French physics researcher in magnetic resonance. The French Society of Radiology wanted to award* Abragam *a medal in spite of the fact that he told them he hadn't contributed to* MRI *and didn't believe it would work.*

Abragam replied: *There was nuclear magnetic resonance before* Erwin Louis Hahn's *discovery of the spin echo, there is nuclear magnetic resonance after. It is not the same.*

The truth is, contrary to some of the preconceived opinions about its evolution, that clinical magnetic resonance tomography is a quickly expanding topic at an extremely rapid pace of innovation.

Understanding the modality of magnetic resonance tomography helps to understand the structure of the Kerr space–time in the sense of Felix Klein's Erlanger Programm. The investigation of its structure is synonymous to black hole research.

2 The Real Heisenberg Lie Group

The quantum holographic approach to conformal steady–state free–precession and magnetic resonance tomography depends on the ordering concept of real Heisenberg Lie group $\mathcal{N}_0 = \mathbb{R} \times \mathbb{R} \times \mathbb{T}$ with the twisted multiplication law

$$(x_1, y_1, z_1)(x_2, y_2, z_2) = (x_1 + x_2, y_1 + y_2, z_1 z_2 \mathbf{e}(x_1 y_2))$$

where, as usual, $\mathbf{e}(\theta) = \exp(2\pi i\theta) = e^{2\pi i\theta}$ for $\theta \in \mathbb{R}$ describes the central phase circle $\mathrm{U}(1, \mathbb{C}) \cong \mathbb{T}$ within the symplectic plane $\mathbb{R} \oplus \mathbb{R} \cong \mathbb{C}_{\mathbb{R}}$ of infinitesimal loop rotation $\Im \frac{\mathrm{d}}{\mathrm{d}\theta} \restriction_{\theta=0} \mathbf{e}(\theta) = 2\pi$.

The symplectic plane $\mathbb{R} \oplus \mathbb{R} \cong \mathbb{C}_{\mathbb{R}}$ and the one–dimensional compact torus group

$$\mathbb{T} \cong \mathbb{R}/\mathbb{Z} \cong \mathrm{U}(1, \mathbb{C}) \cong \mathrm{SO}(2, \mathbb{R})$$

are considered as embedded into $\mathcal{N}_0$. The center of $\mathcal{N}_0$ is $\mathbb{T} \lhd \mathcal{N}_0$. There is an obvious complexification of $\mathcal{N}_0$, which is an extension of $\mathbb{C}_{\mathbb{R}} \cong \mathbb{R}(i) \cong \mathbb{C}$ by $\mathbb{C}^\times$. According to the Stone–von Neumann theorem, the central character

$$\mathbb{R} \ni \theta \rightsquigarrow \mathbf{e}(\nu\,\theta) \in \mathbb{T} \qquad (\nu \in \mathbb{R}^\times)$$

determines by their central Larmor labels $\nu \in \mathbb{R}^\times$ the equivalence classes of irreducible unitary linear representations of $\mathcal{N}_0$. The strong Stone–von Neumann theorem asserts on the L^2 level of the two–sided ideal of Hilbert–Schmidt operators that square integrability modulo the center is valid if and only if unicity by the central character is guaranteed.

To provide geometric insight into the harmonic analysis of $\mathcal{N}_0$, notice that the universal covering group of $\mathcal{N}_0$ is a three–dimensional real Lie group $\mathcal{N}$ which is also called Heisenberg group. The center of $\mathcal{N}$ is $\mathbb{R} \lhd \mathcal{N}$, where the real line $\mathbb{R}$ is conceived as the universal covering group of the one–dimensional compact torus group $\mathbb{T}$. The real Lie algebras $\mathrm{Lie}(\mathcal{N}_0)$ and $\mathrm{Lie}(\mathcal{N})$ coincide, and the real dual vector space

$$\mathrm{Lie}(\mathcal{N}_0)^* \cong \mathrm{Lie}(\mathcal{N})^*$$

gives rise to the affine coadjoint orbit model $\mathrm{Lie}(\mathcal{N})^*/\mathrm{CoAd}(\mathcal{N})$ of the unitary dual of $\mathcal{N}$ which consists of the equivalence classes of irreducible unitary linear representations of $\mathcal{N}$ ([20], [31]). Geometrically, it represents a stack of non–homogeneous affine contact planes and a unique homogeneous singular control plane within the ambient dual vector space $\mathrm{Lie}(\mathcal{N})^*$; see Figures 2 and 3. In magnetic resonance tomography, the slice selection is performed by switching trains of axial linear gradients.

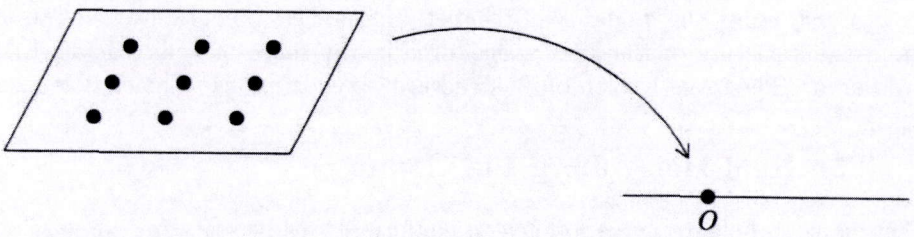

Fig. 2: The boundary plane of the non–Euclidean hyperbolic half–space $\mathbb{P}_3$ forms the unique singular control plane $\nu = 0$ of the affine coadjoint orbit model $\mathrm{Lie}(\mathcal{N})^*/\mathrm{CoAd}(\mathcal{N})$. It consists of Dirac point measures at $w_0 \in \mathbb{C}_{\mathbb{R}}$ which control the canonical holomorphic and antiholomorphic line bundles $L_{\mathbb{C}}$ and $\bar{L}_{\mathbb{C}}$ of the bipolar stereographic projection η. The Dirac measures are in bijective correspondence to the unitary characters of the real Heisenberg Lie group $\mathcal{N}$. In the projective differential geometry of symplectic spinors, the frequency–splitting plane $\nu = 0$ gives rise to the singularity of the stationary, axially symmetric, and asymtotically flat Kerr space–time metric of post–Kepplerian cosmology and its multipolar moment configuration. An extension of the singular plane $\nu = 0$ is the flat Minkowski space–time. © W. Schempp

3 A Relativistic Perspective: The Spin Factor

The real Lie group generated by the conformal Möbius inversions of the Riemannian sphere $\mathbb{S}_2 \cong \mathbb{P}_1(\mathbb{C})$ acting on the three–dimensional real projective space $\mathbb{P}_3(\mathbb{R})$ is given by the projective orthogonal group

$$\mathrm{PO}(3,1,\mathbb{R}) \cong \mathrm{O}(3,1,\mathbb{R})/\{\mathrm{id}, -\mathrm{id}\}\,.$$

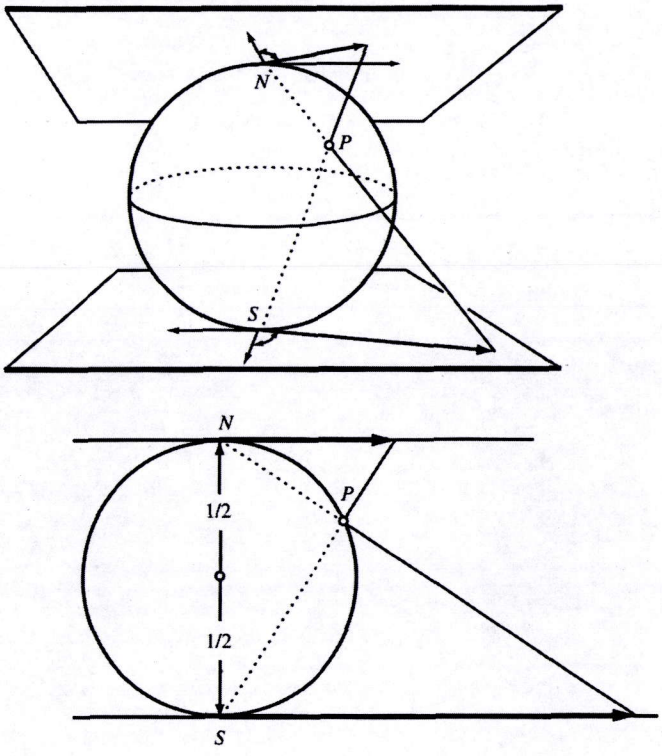

Fig. 3: Conformal projective differential geometry of orthogonality involutions: The modality of bipolar stereographic projection η from the round sphere of diameter 1 in $\mathbb{R}^3$ in the contact geometry of planar coadjoint orbits of the three–dimensional real Heisenberg Lie group $\mathcal{N}$. The Riemann surface $\mathbb{S}_2 \cong \mathbb{P}_1(\mathbb{C})$ is regarded as the union of two affine copies of the plane $\mathbb{C}_{\mathbb{R}}$ with parallel real axes $\mathbb{R}$ and identification performed by the conformal inversion $\kappa : \mathbb{C}_{\mathbb{R}}^{\times} \ni 2\pi i w \rightsquigarrow \frac{1}{2\pi i w} \in \mathbb{C}_{\mathbb{R}}^{\times}$. The manifold of fibers of the Hopf principal bundle $\mathbb{S}_1 \hookrightarrow \mathbb{S}_3 \longrightarrow \mathbb{S}_2$ fit together conformally to represent the two–dimensional round sphere $\mathbb{S}_2 \cong \mathrm{O}(3,\mathbb{R})/\mathrm{O}(2,\mathbb{R})$ in the ambient conformally projectivized dual vector space $\mathrm{PLie}(\mathcal{N})^*$. © W. Schempp

The invariance group $\mathrm{PSO}(3,1,\mathbb{R})$ of inversive plane geometry is isomorphic to the Lorentz group $\mathrm{PSL}(2,\mathbb{C})$ associated with the non–Euclidean hyperbolic half–space $\mathbb{P}_3 \hookrightarrow \mathbb{P}_3(\mathbb{R})$. Let Γ denote the cross–sectional functor, and S, $\wedge$ the symmetrization and skew–symmetrization functors, respectively, of the category of fiber bundles over differentiable manifolds. Then Γ recognizes the fibered structure of the underlying smooth manifold. The projective orthogonal group $\mathrm{PO}(3,1,\mathbb{R})$ associates the cross–

sectional bilinear symmetric two–form fiber

$$-\mathrm{d}r^2 + \mathrm{d}x^2 + \mathrm{d}y^2 + \mathrm{d}z^2 \in \Gamma(\mathrm{S}^2\mathrm{T}^\star\mathbb{R}^4)$$

of Minkowski signature (3,1) on the dual tangent bundle of the real vector space $\mathbb{R}^4$ with positive definite symmetric absolute two–tensor. The group $\mathrm{PO}(3,1,\mathbb{R})$ admits the neutral component

$$\mathrm{PO}_0(3,1,\mathbb{R}) \cong \mathrm{O}_0(3,1,\mathbb{R}).$$

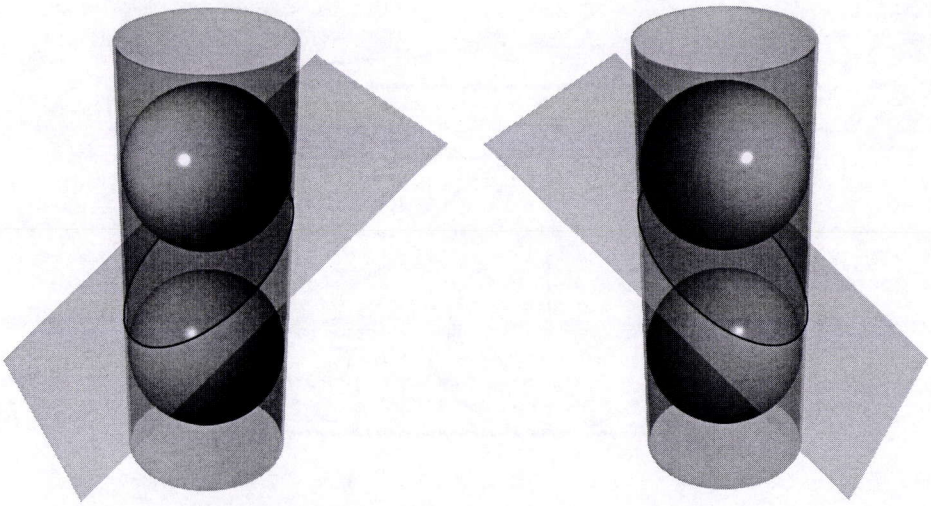

Fig. 4: Stationary contact trajectories performing balanced steady–state free–precession: Generation of the inversive geometry of the affine coadjoint orbit model $\mathrm{Lie}(\mathcal{N})^*/\mathrm{CoAd}(\mathcal{N})$ of the real Heisenberg Lie group $\mathcal{N}$ in the ambient conformally projectivized dual vector space $\mathrm{PLie}(\mathcal{N})^\star$. The center of the real Heisenberg Lie algebra $\mathrm{Lie}(\mathcal{N})$ identifies with the axis of the the axisymmetric Fock–Kähler manifold $\mathbb{S}_2 \times \check{\mathbb{S}}_2 \hookrightarrow \mathbb{C}^2_{\mathbb{R}} \times \mathbb{C}^2_{\mathbb{R}}$. Its direction in $\mathrm{PLie}(\mathcal{N})^\star$ is given by the line of sight. In the detachment case $N = 1$, the gradient switched contact planes of Kähler type (1,0) and (0,1), respectively, are holomorphic and antiholomorphic sections of the tangent bundle $(\mathrm{T}(\mathbb{S}_2 \times \check{\mathbb{S}}_2), \check{J} \otimes_{\mathbb{R}} J)$ which implement contact geometrically the foci. In quantum cosmology the Fock–Kähler manifold $\mathbb{S}_2 \times \check{\mathbb{S}}_2 \hookrightarrow \mathbb{C}^2_{\mathbb{R}} \times \mathbb{C}^2_{\mathbb{R}}$ describes the post–Kepplerian effect of advance of perenigricon. © W. Schempp

The Lie group of orientation preserving conformal Möbius inversions of $\mathbb{P}_3(\mathbb{R})$ is non–compact and isomorphic to the group of automorphisms of the round sphere $\mathbb{S}_2 \cong \mathrm{O}(3,\mathbb{R})/\mathrm{O}(2,\mathbb{R})$. It was this kind of observations in which Arthur Cayley obtained various metrics that led him to state with succinct enthusiasm metric geometry to be subordinate to projective geometry, and projective geometry to

be *all* of geometry. After the development of general relativity theory, projective geometry had to be extended to projective differential geometry in order to describe in quantum cosmology the post–Kepplerian advance of perenigricon, the effect of gravitational radiation damping, causing a measurable rate of orbital decay, and the detection of changes in the pulse shape, resulting from geodetic spin precession of binary pulsars; see Figure 6. The axial and transversal relaxation effects of nuclear spin ensembles in magnetic resonance tomography indicate the important link of quantum cosmology and mathematical radiology.

The spin factor associated with the real Heisenberg Lie group $\mathcal{N} \cong \mathbb{C}_{\mathbb{R}} \oplus \mathbb{R}$ is given by

$$\mathcal{J}(\mathbb{C}_{\mathbb{R}} \oplus \mathbb{R}) \cong \mathbb{C}_{\mathbb{R}} \oplus \mathbb{R} \underbrace{\oplus \mathbb{R}}.$$

It forms a Jordan algebra under the multiplication law induced by the Minkowski metric and therefore is one of the most remarkable in the classification of simple formally real Jordan algebras ([1]). The projective orthogonal group $\mathrm{PO}(3,1,\mathbb{R})$ acts on $\mathcal{J}(\mathbb{C}_{\mathbb{R}} \oplus \mathbb{R})$ as the group of isometries. Its one–dimensional subspaces spanned by non–zero isotropic vectors are the light rays inside the light cone of $\mathcal{J}(\mathbb{C}_{\mathbb{R}} \oplus \mathbb{R})$. The manifold of all light rays is called the heavenly sphere $\mathbb{P}_1(\mathbb{C}) \cong \mathbb{S}_2$ of the spin factor $\mathcal{J}(\mathbb{C}_{\mathbb{R}} \oplus \mathbb{R})$ associated with $\mathcal{N}$. If the symplectic spinors are restricted to the multiplicative Lie group $\mathrm{SU}(2,\mathbb{C}) \cong \mathrm{Spin}(3,\mathbb{R}) \cong \mathbb{S}_3$ of unit quaternions, the Hopf projector

$$\eta : \mathbb{S}_3 \longrightarrow \mathbb{S}_2$$

pops up. The Taub manifold $\mathbb{R} \times \mathbb{S}_3$ should then be seen in connection with cosmology ([17])). To quote Jean–Marie Souriau:

La variété de Képler est globalement symplectomorphe au fibré cotangent à la sphère $\mathbb{S}_3$*, privé de sa section nulle.*

Thus, due to the Newtonian approach, the Kepplerian manifold can be symplectomorphically represented by the fiber bundle $(\mathrm{T}^*\mathbb{S}_3)^\times$ ([36], [37]).

The Möbius inversion transforms conformally the affine coadjoint orbit model $\mathrm{Lie}(\mathcal{N})^*/\mathrm{CoAd}(\mathcal{N})$ onto the axisymmetric Fock–Kähler manifold $\mathbb{S}_2 \times \check{\mathbb{S}}_2 \hookrightarrow \mathbb{C}^2_{\mathbb{R}} \times \mathbb{C}^2_{\mathbb{R}}$. It consists of the bicylindrical Dupin cyclide of the projective symplectic orbiton/spinon dynamics laboratory under its principal fibration by circles; see Figures 2 and 3.

4 Momentum Mappings

For the steady–state free–precession the balancing condition reads $2\pi\nu = 1$. The central frequency inversion

$$\mathbb{R}^\times \ni 2\pi\,\nu \rightsquigarrow -2\pi\,\nu \in \mathbb{R}^\times$$

is *logarithmically* associated with the contragredient coadjoint orbit identification mapping

$$\kappa : \mathbb{C}_{\mathbb{R}}^{\times} \ni 2\pi\, i\, w \rightsquigarrow \frac{1}{2\pi\, i\, w} \in \mathbb{C}_{\mathbb{R}}^{\times}$$

of the Hopf principal fibration quantum gate $\mathbb{S}_1 \hookrightarrow \mathbb{S}_3 \longrightarrow \mathbb{S}_2$. The conformal inversion κ may be regarded as arising from two bipolar stereographic projections from the round sphere of radius $\frac{1}{2}$ in $\mathbb{R}^3$. Let $\check{\mathbb{S}}_2 \hookrightarrow \mathbb{R}^3$ denote the round sphere $\mathbb{S}_2 \hookrightarrow \mathbb{R}^3$ endowed with the reverse orientation. The Hermitian metric

$$H = (\cdot|\cdot)_2 + i\,\Omega$$

on the complex tangent bundle $\mathrm{T}(\mathbb{S}_2 \times \check{\mathbb{S}}_2)$, admitting the differential two–form of rotations of reverse orientations as its imaginary part

$$\Omega = \mathrm{d}x_1 \wedge \mathrm{d}y_1 + (-1) \cdot \mathrm{d}y_2 \wedge \mathrm{d}x_2 = \mathrm{d}x_1 \wedge \mathrm{d}y_1 + \mathrm{d}x_2 \wedge \mathrm{d}y_2\,,$$

gives rise to an extension ∇ of the Levi–Civita connection of the Riemannian metric $(\cdot|\cdot)_2$ which pops up as the real part $\Re H$ of the Hermitian metric. Then ∇ is Hermitian with respect to complex tangent vectors (W_1, W_2) of the four–dimensional compact Fock–Kähler manifold $\mathbb{S}_2 \times \check{\mathbb{S}}_2 \hookrightarrow \mathbb{C}_{\mathbb{R}}^2 \times \mathbb{C}_{\mathbb{R}}^2$, and is the unique Hermitian connection of Kähler type (1,0) ([43]).

In the context of an application of the seesaw pair detachment diagram to the tangential spinor structure of $\mathbb{S}_2 \times \check{\mathbb{S}}_2 \hookrightarrow \mathbb{C}_{\mathbb{R}}^2 \times \mathbb{C}_{\mathbb{R}}^2$, the sum of squares factorization

$$\begin{aligned}(x_1y_2 + x_2y_1)^2 + (x_1y_1 - x_2y_2)^2 &= (x_1y_2 - x_2y_1)^2 + (x_1y_1 + x_2y_2)^2 \\ &= (x_1^2 + x_2^2)(y_1^2 + y_2^2),\end{aligned}$$

generates the pair (∇_1, ∇_2) of quantum entangled momentum mappings

$$\nabla_1 : \mathbb{R}^4 \ni \begin{pmatrix} x_1 \\ y_1 \\ x_2 \\ y_2 \end{pmatrix} \rightsquigarrow \begin{pmatrix} x_1y_2 + x_2y_1 \\ \frac{1}{2}(x_1^2 + x_2^2) \\ x_1y_1 - x_2y_2 \\ \frac{1}{2}(y_1^2 + y_2^2) \end{pmatrix} \in \mathbb{R}^4$$

$$\nabla_2 : \mathbb{R}^4 \ni \begin{pmatrix} x_1 \\ y_1 \\ x_2 \\ y_2 \end{pmatrix} \rightsquigarrow \begin{pmatrix} x_1y_2 - x_2y_1 \\ \frac{1}{2}(x_1^2 + x_2^2) \\ x_1y_1 + x_2y_2 \\ \frac{1}{2}(y_1^2 + y_2^2) \end{pmatrix} \in \mathbb{R}^4,$$

which are acting equivariantly under the coadjoint action CoAd of the real Heisenberg Lie group $\mathcal{N}$ on the four–dimensional compact Fock–Kähler product manifold

$$(\mathbb{S}_2 \times \check{\mathbb{S}}_2, \Omega).$$

Due to the isomorphy of groups

$$\mathrm{O}(2,\mathbb{R}) \cap \mathrm{Sp}(2,\mathbb{R}) \cong \mathrm{U}(1,\mathbb{C}),$$

the ranges of the quantum entangled momentum mappings ∇_1 and ∇_2 are circular cones on the two–dimensional compact spheres $\mathbb{S}_2 \hookrightarrow \mathbb{R}^3$ and $\check{\mathbb{S}}_2 \hookrightarrow \mathbb{R}^3$, respectively. The parallel symplectic differential two–form Ω is closed and yields, according to the third Kepplerian law, the conditions for the entangled energy level geometric quantization of the compact Fock–Kähler manifold $\mathbb{S}_2 \times \check{\mathbb{S}}_2 \hookrightarrow \mathbb{C}^2_{\mathbb{R}} \times \mathbb{C}^2_{\mathbb{R}}$ of stationary contact trajectories.

5 Linear Gradient Bundles and Isotropic Lines

To understand topologically the post–Kepplerian effect of perenigricon advance, recall that in terms of projective contact geometry any point of a central conic in which conjugate lines are orthogonal is called a *focus* of the tangential spinor structure. Because a focus is never located on the conic itself, it admits two different tangent lines which are invariant under the action of the *orthogonality involution.* Each tangent line is conjugate to itself, so that the tangents are *isotropic* lines and therefore pass through the absolute circular points

$$\varepsilon_1 = (1, -i, 0), \qquad \varepsilon_2 = (1, i, 0)$$

on the zero–dimensional absolute quadric

$$x^2 + y^2 = w\,\bar{w} = |w|^2 = z = 0$$

of the complex projective plane $\mathbb{P}_2(\mathbb{C})$. Motivated by the pair (∇_1, ∇_2) of quantum entangled momentum mappings, consider $\mathbb{P}_2(\mathbb{C})$ as the projective closure of the Euclidean plane $\mathbb{R} \oplus \mathbb{R} \cong \mathbb{C}_{\mathbb{R}}$. Due to Edmond Nicolas Laguerre's cross ratio based phase formula it follows:

Theorem 2. *In the Euclidean plane $\mathbb{R} \oplus \mathbb{R}$, a projectivity of a linear gradient bundle that leaves fixed its two isotropic lines is induced by a planar rotation. The angle of this rotation is a right angle if and only if the projectivity forms an involution, the orthogonality involution.*

The absolute quadric belongs projectively to the the axisymmetric Dupin cyclide which is associated with the canonical parallel almost complex structures

$$J \in \Gamma(\mathrm{End}\,\mathrm{T}(\mathbb{C}^2_{\mathbb{R}})), \qquad \check{J} = -J \in \Gamma(\mathrm{End}\,\mathrm{T}(\mathbb{C}^2_{\mathbb{R}})).$$

They are integrable and admit the matrix form of orthogonality involutions

$$J = \begin{pmatrix} 0 & -1 \\ 1 & 0 \end{pmatrix} \in \mathrm{SL}(2,\mathbb{R}), \qquad \check{J} = \begin{pmatrix} 0 & 1 \\ -1 & 0 \end{pmatrix} \in \mathrm{SL}(2,\mathbb{R})$$

Thus the orthogonalty involution admit the spectrum $\{-i, i\}$. In this context, J is the infinitesimal generator of the maximal compact subgroup $\mathrm{SO}(2,\mathbb{R})$ of $\mathrm{SL}(2,\mathbb{R})$ and the axisymmetric Dupin cyclide is conceived as a principal $\mathrm{U}(1,\mathbb{C})$ fiber bundle. An easy computation shows that the curvature tensor $R \in \Gamma(\mathrm{End}\, \wedge^2 \mathrm{T}(\mathbb{S}_2 \times \check{\mathbb{S}}_2))$ is skew–Hermitian with respect to the Hermitian metric $H = \Omega(\check{J}\cdot, J\cdot) + i\,\Omega$ of the complex connection ∇ in the complex tangent bundle $(\mathrm{T}(\mathbb{S}_2 \times \check{\mathbb{S}}_2), \check{J} \otimes_{\mathbb{R}} J)$. Notice that in a continuous quasi–simple representation of $\mathrm{SL}(2,\mathbb{R})$, the matrices J and $\check{J}$ act diagonally with eigenvalues in the purely imaginary discrete spectrum $i\mathbb{Z}$. For the balanced steady–state free–precision and the pair (∇_1, ∇_2) of quantum entangled momentum mappings, the curvature tensor R reduces to the identity mapping

$$R : (W_1, W_2) \rightsquigarrow W_1 \wedge W_2$$

Multiplication by the imaginary unit i in $\mathbb{C}^2_{\mathbb{R}}$ corresponds to left multiplication by J, and similarly multiplication by $-i$ corresponds to left multiplication by $\check{J}$, to give rise to the almost complex structure $\check{J} \otimes_{\mathbb{R}} J$ of the compact Fock–Kähler manifold $\mathbb{S}_2 \times \check{\mathbb{S}}_2 \hookrightarrow \mathbb{C}^2_{\mathbb{R}} \times \mathbb{C}^2_{\mathbb{R}}$ ([43]). Therefore the focal points are the intersection of the tangent lines of the conic passing through the absolute circular points. Due to the involution of complex conjugation $w \rightsquigarrow \bar{w}$, it is this property which characterizes projectively a focal point. Notice, however, that the compact complex manifold $\mathbb{S}_3 \times \check{\mathbb{S}}_3$ is not a Kählerian manifold.

6 Canonical Complex Line Bundles and Focal Points

Let $L_{\mathbb{C}}$ denote the canonical holomorphic line bundle of the Riemannian sphere $\mathbb{S}_2 \cong \mathbb{P}_1(\mathbb{C})$ under its standard atlas consisting of two coordinate charts, and $\bar{L}_{\mathbb{C}}$ its antiholomorphic counterpart. As real vector bundles, $L_{\mathbb{C}}$ and $\bar{L}_{\mathbb{C}}$ have dimension 2. They can be constructed by taking trivial bundles over the northern and southern hemispheres of $\mathbb{S}_2 \hookrightarrow \mathbb{R}^3$ and $\check{\mathbb{S}}_2 \hookrightarrow \mathbb{R}^3$, respectively, with *two* trivializations of the fiber over the points on the equator. Gluing the trivial bundles together along the equator results in the mapping

$$\mathbb{S}_1 \longrightarrow \mathrm{O}(2,\mathbb{R})$$

which is sending any element of $\mathbb{C}_{\mathbb{R}}$ of absolute value 1 to the operation of right–handed multiplication with the phase factor. A similar argument holds for the left–handed mutiplication with the inverse phase factor

$$\check{\mathbb{S}}_1 \longrightarrow \mathrm{O}(2,\mathbb{R}).$$

The homotopy classes of these mappings generate the homotopy group

$$\pi_1(\mathrm{O}(2,\mathbb{R})) \cong \mathbb{Z}.$$

Jointly together, the twisted action

$$\mathbb{T} \times \mathbb{T} \longrightarrow \mathrm{O}(2,\mathbb{R}) \times \mathrm{O}(2,\mathbb{R})$$

completes the bottom line of the seesaw pair detachment diagram supra, and inserts principal $\mathbb{Z}_2$ bundle of the Villarceau bounded Möbius strips into the Hopf principal bundle $\mathbb{S}_1 \hookrightarrow \mathbb{S}_3 \longrightarrow \mathbb{S}_2$; see Figure 5.

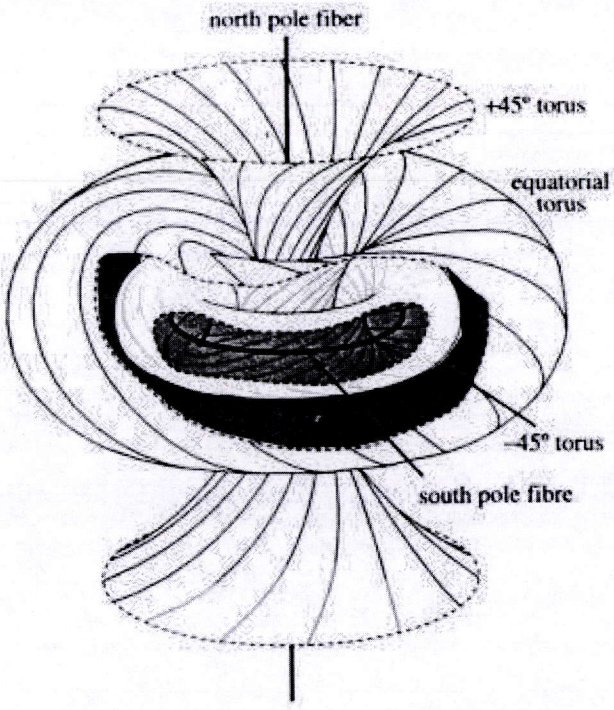

Fig. 5: Post–Kepplerian orbiton/spinon dynamics: The $L_{\mathbb{C}} \otimes \bar{L}_{\mathbb{C}}$ canonical line bundle methodology of the Fock–Kähler manifold $\mathbb{S}_2 \times \check{\mathbb{S}}_2 \hookrightarrow \mathbb{C}^2_{\mathbb{R}} \times \mathbb{C}^2_{\mathbb{R}}$ gives rise to the Hopf fibration $\mathbb{S}_1 \hookrightarrow \mathbb{S}_3 \longrightarrow \mathbb{S}_2$ and the circular traces of the Villarceau bounded Möbius $\mathbb{Z}_2$ bundle. The seesaw pair configuration acts on the Villarceau phase circles of the round sphere $\mathbb{S}_3 \cong \mathrm{Spin}(3, \mathbb{R})$ through phase shifting. © W. Schempp

A closely related perspective on the canonical line bundles $L_{\mathbb{C}}$ and $\bar{L}_{\mathbb{C}}$ comes from looking at the associated unit circle bundles. Any fiber of $L_{\mathbb{C}}$ carries a scalar product, since it forms a line through the origin in $\mathbb{C}^2_{\mathbb{R}}$. The unit circle in each fiber generates a bundle of phase circles $\mathbb{S}_1$ over the Riemann surface $\mathbb{P}_1(\mathbb{C})$ called the Hopf bundle:

$$\eta : \mathbb{S}_3 \longrightarrow \mathbb{P}_1(\mathbb{C})$$

The total manifold $\mathbb{S}_3 \cong \mathrm{Spin}(3, \mathbb{R})$ consists of all the unit vectors in $\mathbb{C}^2_{\mathbb{R}}$, the base manifold $\mathbb{P}_1(\mathbb{C})$ can be described in terms of lines through the origin. The pre–image

$$\{\eta^{-1}(\varepsilon_1), \eta^{-1}(\varepsilon_2)\}$$

of the absolute circular points $\{\varepsilon_1, \varepsilon_2\}$ under the Hopf projector η is a pair of *linked* phase circles in the sphere $\mathbb{S}_3 \cong \mathrm{Spin}(3, \mathbb{R})$, which form the famous Hopf link of Clifford parallel Villarceau phase circles of the first and second kind in $\mathbb{R}^4$ ([39]). An analogous argument holds for the line bundle $\bar{L}_{\mathbb{C}}$. The line bundles $L_{\mathbb{C}}$ and $\bar{L}_{\mathbb{C}}$ implement in the axisymmetric Fock–Kähler manifold $\mathbb{S}_2 \times \check{\mathbb{S}}_2 \hookrightarrow \mathbb{C}^2_{\mathbb{R}} \times \mathbb{C}^2_{\mathbb{R}}$ the post–Kepplerian perenigricon effect.

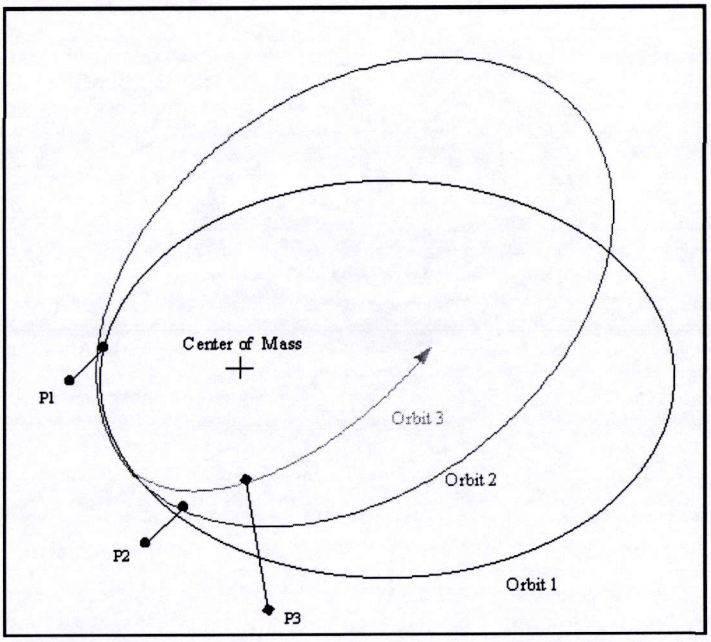

Fig. 6: Post–Kepplerian orbiton/spinon dynamics: The tangential Hopf link of three stationary trajectories of a relativistic binary pulsar surrounding the center of mass. The positions indicate the local phase advance at perenigricon. The local phase shift at perenigricon derives from the twisted action $\mathbb{T} \times \mathbb{T} \longrightarrow \mathrm{O}(2, \mathbb{R}) \times \mathrm{O}(2, \mathbb{R})$ on the seesaw pair detachment diagram. © W. Schempp

Let $\mathcal{H}^0(\mathbb{S}_2, L_{\mathbb{C}})$ denote the Riemann–Roch vector space over the field $\mathbb{C}$ of holomorphic sections of $L_{\mathbb{C}}$ over the compact symplectic manifold $\mathbb{S}_2 \hookrightarrow \mathbb{C}^2_{\mathbb{R}}$, and $\mathcal{H}^0(\check{\mathbb{S}}_2, \bar{L}_{\mathbb{C}})$ the corresponding Riemann–Roch vector space over $\mathbb{C}$ of antiholomorphic sections of $\bar{L}_{\mathbb{C}}$ over the compact symplectic manifold $\check{\mathbb{S}}_2 \hookrightarrow \mathbb{C}^2_{\mathbb{R}}$ under the reverse orientation. In terms of sheaf theory, $\mathcal{H}^0(\mathbb{S}_2, L_{\mathbb{C}})$ and $\mathcal{H}^0(\check{\mathbb{S}}_2, \bar{L}_{\mathbb{C}})$ are known as the cohomology groups of $\mathbb{S}_2$ and $\check{\mathbb{S}}_2$ with coefficients in the sheaf of germs of holomorphic and antiholomorphic sections of the holomorphic and antiholomorphic line bundles $L_{\mathbb{C}}$ and $\bar{L}_{\mathbb{C}}$, respectively ([43], [19]). A holomorphic plane is referred to as self–dual, and a antiholomorphic plane as anti–self–dual.

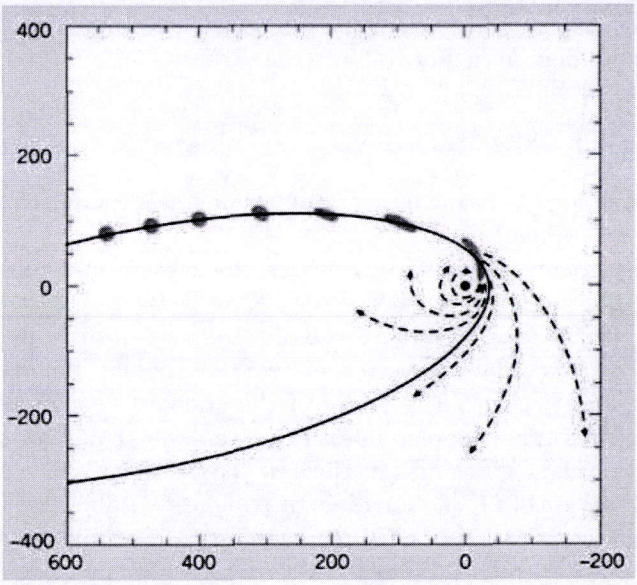

Fig. 7: Laboratory of post–Kepplerian orbiton/spinon dynamics: A gas cloud on its way towards the supermassive black hole at the center Sagittarius A* of the Milky Way galaxy. The cloud becomes elongated because of the tidal force acting on it, especially as it nears the perenigricon where it is violently sheared and the trajectories of different branches of the cloud diverge. The diagram displays the angular offsets from the central black hole in right ascension and declination in units of milliarcseconds, and the post–Kepplerian equilibrium state. © W. Schempp

In view of the horizontal N–level quantization condition ([35])

$$\frac{1}{2}\dim_{\mathbb{C}} \mathcal{H}^0(\mathbb{S}_2 \times \check{\mathbb{S}}_2, L_{\mathbb{C}} \otimes \bar{L}_{\mathbb{C}}) = (N+1)^2 \qquad (N \in \mathbb{N}),$$

the critical point condition of the energy functional through the Euler–Lagrange equations of contact geometry yields in terms of the canonically complexified differential operators

$$\partial = \frac{\partial}{\partial w} = \frac{1}{2}(\frac{\partial}{\partial x} - i\frac{\partial}{\partial y}) = \frac{1}{2}(\frac{\partial}{\partial x} - iJ\frac{\partial}{\partial x})$$

where $w = x + iy \in \mathbb{C}_{\mathbb{R}}$, and

$$\bar{\partial} = \frac{\partial}{\partial \bar{w}} = \frac{1}{2}(\frac{\partial}{\partial x} + i\frac{\partial}{\partial y}) = \frac{1}{2}(\frac{\partial}{\partial x} + i\check{J}\frac{\partial}{\partial x})$$

the Cauchy–Riemann equations for the germs of holomorphic and respectively anti-holomorphic functions on the planar affine coadjoint orbit model $\mathrm{Lie}(\mathcal{N})^*/\mathrm{CoAd}(\mathcal{N})$.

In the case of continuously differentiable functions, Stokes' formula adds to the mapping κ the linear gradient kernel of Kähler type (1,0)

$$\frac{1}{2\pi i} \cdot \frac{\bar{\partial}}{w - w_0} \, \mathrm{d}w \wedge \mathrm{d}\bar{w} \qquad (w_0 \in \mathbb{C}_{\mathbb{R}}).$$

The switching of gradient recalled echoes determines the performance of clinical magnetic resonance scanners.

Due to the diagonal action of $-i\check{J}$ under the metaplectic representation of $\mathrm{Mp}(2,\mathbb{R})$ with eigenvalues in the discrete set $\mathbb{Z} \cong \pi_1(\mathrm{O}(2,\mathbb{R}))$, it admits *at attachment* the Kepplerian energy level $N = 0$ of the lowest positive weight $\frac{1}{2}$ of even functions in the complex Schwartz vector space $\mathcal{S}(\mathbb{R})$. This is in correspondence to the unique focal point which is the center of the circular Kepplerian contact trajectory counted twice. The Kepplerian energy level $N = 1$ admits *at detachment* the lowest positive weight $\frac{3}{2}$ of odd functions in the Schwartz space $\mathcal{S}(\mathbb{R})$. For the diagonal $\mathrm{Mp}(2,\mathbb{R})$ action of iJ, the corresponditg highest weights are $-\frac{1}{2}$ and $-\frac{3}{2}$, respectively. The characterization of focal points in terms of orthogonality involutions provide contact geometrically 4 different entangled foci of the corresponding non–circular central Kepplerian contact trajectory of quantum cohomology; see Figure 4.

Theorem 3. *The quantum entangled foci are pairwise conjugate points in symmetric position with respect to the center. Two of the focal points are real and located on the first axes, and the other two are non–real and located on the second axes. Their momenta can be read off from the quantum entangled momentum mappings* (∇_1, ∇_2).

Let $a > 0$ denote the major and $b > 0$ the minor semi–axis of the central Kepplerian contact trajectory. In terms of the linear excentricity $\sqrt{a^2 - b^2}$, the corresponding foci admit the homogeneous coordinates

$$(1, 0, \pm\sqrt{a^2 - b^2}), \quad (1, \pm i\sqrt{a^2 - b^2}, 0) \qquad (a > b > 0)$$

in the complex projective plane $\mathbb{P}_2(\mathbb{C})$.

Corollary 1. *The two real or imaginary foci determine the other two in terms of the linear excentricity.*

The holomorphic focal realization follows by the convolutional contour integral over the germ of the Nth–order derivative of the Cauchy reproducing kernel

$$\kappa^{(N)} = \frac{N!}{2\pi i} \cdot \frac{1}{(w - w_0)^{N+1}} \, \mathrm{d}w \qquad (w_0 \in \mathbb{C}_{\mathbb{R}}, N \in \{0, 1\}).$$

It results from the polarization identification map κ of the Hopf principal fibration quantum gate $\mathbb{S}_1 \hookrightarrow \mathbb{S}_3 \longrightarrow \mathbb{S}_2$ by a focal shift of order $N \in \{0, 1\}$ linearization. Remarkably, the Cauchy integral formula along a null–homological path pops up in

1831 within the field of celestial mechanics. Indeed, the lithographic treatise of the member of the *Académie de Turin*, Augustin Louis Cauchy, Professor of Astronomy at the Sorbonne, has been entitled *"Sur la mécanique céleste et sur un nouveau calcul appelé calcul des limites"*. Equivalently, because the metaplectic representation of $\mathrm{Mp}(2,\mathbb{R})$ projects the almost complex structure J onto the Fourier cotranform $\bar{\mathcal{F}}_{\mathbb{R}}$ and $\check{J}$ onto the Fourier transform $\mathcal{F}_{\mathbb{R}}$ of cyclic spectrum

$$\{1,-i,-1,i\}$$

by the design of a Fourier filter–bank of order 4. Transition from $\bar{\mathcal{F}}_{\mathbb{R}}$ to the symplectic Fourier transform allows to reduce the order to 2. This is the reason for the pun "blackholography" of adapting the quantum holographic reconstruction procedure to the high resolution imaging of the surrounding cosmological laboratories of black holes; see Figure 8. Due to the the seesaw pair detachment configuration, the tangential Hopf link implies for the post–Kepplerian orbiton/spinon dynamics:

Corollary 2. *The stationary contact trajectories admit a local phase shift at perenigricon.*

There is a discrete phase shift analogy to the Gouy effect of phase coherent optics which is explained by means of the Maslov index.

7 Spectral Theory and the Third Kepplerian Law

The orbiton/spinon dynamics of the balanced steady–state free–precession combined with the automorphic scattering theory yields the extremally weighted, irreducible $\mathrm{Lie}(\mathrm{SL}(2,\mathbb{R}))$ eigenmodule $\mathbb{Z}_2 \times \mathbb{Z}_2$ graduation

$$\left(\mathcal{M}_{-\frac{3}{2}}\hat{\otimes}\bar{\mathcal{M}}_{\frac{1}{2}}, \mathcal{M}_{\frac{3}{2}}\hat{\otimes}\bar{\mathcal{M}}_{-\frac{1}{2}}\right)$$

of the complex vector space of tempered Schwartz distributions

$$\mathcal{S}'(\mathbb{R})\hat{\otimes}\mathcal{S}'(\mathbb{R}) \cong \mathcal{S}'(\mathbb{R}\oplus\mathbb{R})$$

on the real symplectic plane $\mathbb{R}\oplus\mathbb{R} \cong \mathbb{C}_{\mathbb{R}}$. The action of the projective orthogonal group $\mathrm{PO}(3,1,\mathbb{R})$ induces the third Kepplerian law outlined in the great *Harmonices Mundi* of 1619: According to the hyperbolic distance of inversive plane geometry, the third power of the major semi–axis $a > 0$ of the Kepplerian ellipse is proportional to the product of the square of the timing of oriented revolution

$$T = \frac{1}{2\pi\nu} \qquad (\nu \in \mathbb{R}^{\times})$$

and the mass m_0 of the central object. The seesaw pair configuration implies the spectral decomposition of the complex vector space $\mathcal{S}'(\mathbb{R} \oplus \mathbb{R})$. It follows the *ratio orbium*, the reciprocal Schwarzschild–Kepplerian proportions of Heisenberg rotations

$$\left\{\frac{m_0 T^2}{a^3}, \frac{a^3}{m_0 T^2}\right\}$$

which permits to derive the mass of the object located at the focus of the Kepplerian ellipse and hence to incontrovertibly establish the existence of the supermassive black hole Sagittarius A* in the center of the Milky Way galaxy ([11], [13]).

Keppler, the radical Copernican, was so excited by the ecstatic truth of his fundamental discovery that he immediately added the following lines of enthusiasm to the introduction of Book V of *Harmonices Mundi* of 1619:

Now, since the dawn eight months ago, since the broad daylight three months ago, and since a few days ago, when the full Sun illuminated my wonderful speculations, nothing holds me back. I yield freely to the sacred frenzy; I dare frankly to confess that I have stolen the golden vessels of the Egyptians to build a tabernacle for my God far from the bounds of Egypt. If you pardon me, I shall rejoice; if you reproach me, I shall endure. The die is cast, and I am writing the book - to be read either now or by posterity, it matters not. I can wait a century for a reader, as God himself has waited six thousand years for a witness.

Actually, Keppler had to wait much more than a century for the acceptance of his astrophysical breakthrough.

8 Quantum Entanglement and Spin Echoes

According to the projective classification of involutive motions as central collineations in the metaplectic geometry of the affine coadjoint orbit model $\mathrm{Lie}(\mathcal{N})^*/\mathrm{CoAd}(\mathcal{N})$ of the real Heisenberg Lie group $\mathcal{N}$ within the ambient conformally projectivized dual vector space $\mathrm{PLie}(\mathcal{N})^*$, the main difference between the phenomena of gradient recalled echo and spin echo consists in the fact, that the gradient recalled echo occurs by complex conjugation inside the same tomographic slice, whereas quantum entangled spin echoes are phase *coherently* created by unipolar stereographic projection across the foliation of planar coadjoint orbits from the cogredient to the associated contragedient orbit of $\mathcal{N}$ in $\mathrm{Lie}(\mathcal{N})^*$ of inverse central Larmor label.

In terms of the realization of the affine coadjoint orbit model $\mathrm{Lie}(\mathcal{N})^*/\mathrm{CoAd}(\mathcal{N})$ of $\mathcal{N}$ by the Hopf principal fibration quantum gate over the complex projective line $\mathbb{P}_1(\mathbb{C}) \cong \mathbb{S}_2$, the visualizaion of quantum entangled spin echoes is geometrically performed by the concept of Clifford parallelism of flat equatorial tori based Villarceau phase circles of the first and second kind; see Figure 5. The Hopf links consisting of the linked Villarceau phase circles which are coherently embedded into the round sphere $\mathbb{S}_3 \cong \mathrm{O}(4,\mathbb{R})/\mathrm{O}(3,\mathbb{R}) \cong \mathrm{Spin}(3,\mathbb{R}) \cong \mathrm{SU}(2,\mathbb{C})$ visualize the phenomenon of quantum entangled spin echoes.

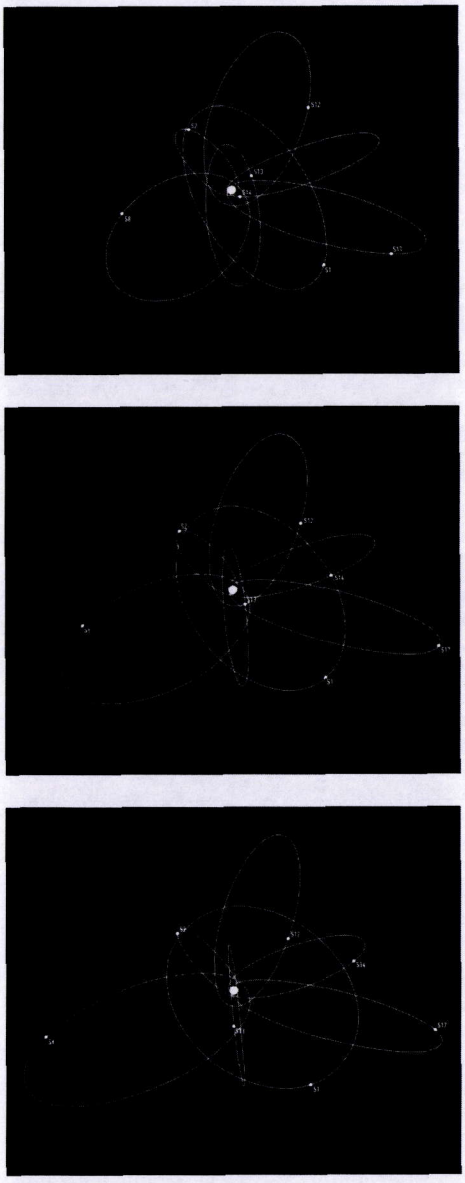

Fig. 8: Projective differential geometry: The Kepplerian orbiton/spinon dynamics of balanced steady–state free–precession. The ray–tracing simulation based on the data from observations illustrates the highly excentric planar trajectoriess of the nuclear stellar cluster steadily precessing around the central supermassive black hole Sagittarius A* of the galaxis. Due to the cosmic dust, the interpolatory data of the focal bundle of inversive planes are obtained by long term high resolution observation by a laser guide stellar adaptive optics system in the near–infrared region. A mirror in the telescope moves constantly to correct for the effect of turbulence in the earth's atmosphere. © W. Schempp

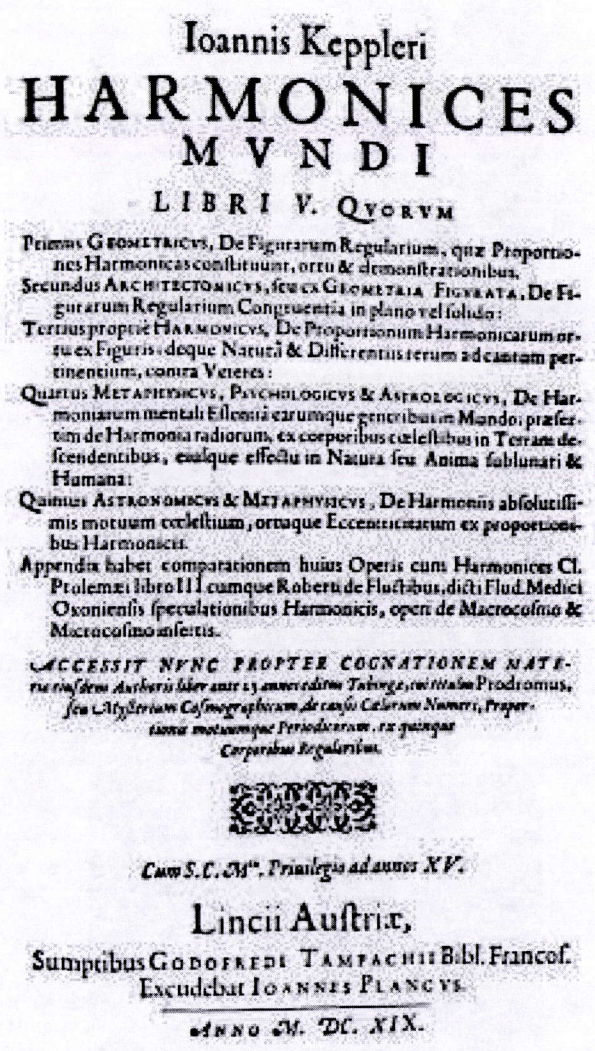

Ioannis Keppleri

HARMONICES MVNDI

LIBRI V. QVORVM

Primus GEOMETRICVS, De Figurarum Regularium, quæ Proportiones Harmonicas constituunt, ortu & demonstrationibus.

Secundus ARCHITECTONICVS, seu ex GEOMETRIA FIGVRATA, De Figurarum Regularium Congruentia in plano vel solido:

Tertius proprie HARMONICVS, De Proportionum Harmonicarum ortu ex Figuris: deque Naturâ & Differentiis rerum ad cantum pertinentium, contra Veteres:

Quartus METAPHYSICVS, PSYCHOLOGICVS & ASTROLOGICVS, De Harmoniarum mentali Essentiâ earumque generibus in Mundo; præsertim de Harmonia radiorum, ex coeporibus cœlestibus in Terram descendentibus, eaque effectu in Natura seu Anima sublunari & Humana:

Quintus ASTRONOMICVS & METAPHYSICVS, De Harmoniis absolutissimis motuum cœlestium, ortuque Eccentricitatum ex proportionibus Harmonicis.

Appendix habet comparationem huius Operis cum Harmonices Cl. Ptolemæi libro III cumque Roberti de Fluctibus, dicti Flud Medici Oxoniensis speculationibus Harmonicis, operi de Macrocosmo & Microcosmo insertis.

ACCESSIT NVNC PROPTER COGNATIONEM MATERIÆ ejusdem Auctoris liber ante 13 annos editus Tubingæ, cui titulus Prodromus, seu Mysterium Cosmographicum, de causis Cælorum Numeri, Proportionæ motuumque Periodicorum, ex quinque Corporibus Regularibus.

Cum S. C. Mtis. Privilegio ad annos XV.

Lincii Austriæ,

Sumptibus GODOFREDI TAMPACHII Bibl. Francof.

Excudebat IOANNES PLANCVS.

ANNO M. DC. XIX.

Fig. 9: Kepplerian orbiton/spinon dynamics: The third Kepplerian law of planetary motion followed the first and second law in the great *Harmonices Mundi* of 1619. It determined the control fundament for the surrounding cosmological laboratories of black holes. The incomprehension of later generations have left Keppler's work on the cosmic harmonies in the obscurity he foresaw in the Proemium to Book Five *Astronomicus & Metaphysicus*. It is a wonderful experience to recognize that the sophisticated ordering principles of the Kepplerian *Harmoniis absolutissimis motuum cœlestium* is realized by means of the magnetic resonance scanner.

9 Conclusions

It is an amazing fact that there are roughly 10^{20} rotating black holes in the observable universe ([27], [46]). The extension of the Copernican revolution which replaced the geocentric model by the heliocentric system replaces the sun by the supermassive black hole Sagittarius A* at the center of the Milky Way galaxy.

The unitarily Lie($\mathrm{SL}(2,\mathbb{R})$) derived two–sheeted metaplectic representation of the metaplectic Lie group $\mathrm{Mp}(2,\mathbb{R})$ provides a projective geometrical orbiton/spinon test of Kepplerian spectral type to establish in the vein of quantum blackholography the existence of the supermassive black hole, known as Sagittarius A*, at the center of the Milky Way galaxy. It may not be the most massive, nor the most energetic, but it is by far the closest, only 8 kpc away, and therefore accessible. Its mass is about $4.4 \times 10^6\,\mathrm{M}_\odot$. Reinhard Genzel describes this result of 16 years of high resolution monitoring nuclear stellar clusters as follows:

From the analysis of the orbits of more than two dozen stars and from measurements of the size and motion of the central compact radio source, Sagittarius A*, *current evidence is presented that this radio source must be a massive black hole of about* $4.4 \times 10^6\,\mathrm{M}_\odot$, *beyond any reasonable doubt.*

Unfortunately, the center of the Galaxis is located behind 30–50 magnitudes of visual extinction and characterized by an extreme source density at all wavelengths, which create great observational difficulties in measuring the mean spectral energy distribution of Sagittarius A*. The observations at near–infrared wavelengths need quantum holography as an efficient technique for image reconstruction. Indeed, the point spread function can be conceived as a tracial coefficient function of the irreducible unitary linear representations of the real Heisenberg Lie group $\mathcal{N}$ associated to the affine coadjoint orbit models $\mathrm{Lie}(\mathcal{N})^*/\mathrm{CoAd}(\mathcal{N})$. The technique of quantum holographic reconstruction is one of the features common to imaging the nuclear stellar cluster of the supermassive black hole Sagittarius A* at the center of the Milky Way galaxy and clinical magnetic resonance tomography ([34]).

One of the stars in the stellar cluster, designated as S2, is some 15 times more massive and seven times larger than the sun. The loci defining its trajectory trace a perfect Kepplerian ellipse with one real focus at the position of the supermassive black hole ([27], [46]). It was located at perenigricon a mere 17 light hours away from the central black hole which is roughly three times the distance between the sun and Pluto., while traveling with a speed in excess of 5000 km/s. These measurements were the most extreme ones ever made for such a trajectory and velocity; see Figure 8.

The $4.4\times10^6\,\mathrm{M}_\odot$ of the supermassive central black hole Sagittarius A* is relatively small as compared to the recently observed $17 \times 10^9\,\mathrm{M}_\odot$ of the over–supermassive black hole in the center of the compact lenticular galaxy NGC 1277 ([42]). The symplectic spinor has been observed by high resolution Hubble Space Telescope imaging. The distance of NGC 1277 to the Milky Way galaxy is about 220×10^6

light years.

Supermassive black holes have generally been recognized as the most destructive force in nature. But in recent years, they have undergone a dramatic shift in paradigm. These objects may have been critical to the formation of structure in the early universe, spawning bursts of star formation and nucleating proto–galactic condensations. Possibly half of all the radiation generated after the big bang may be attributed to them, whose number is known to exceed 300 million ([46]).

The discovery of radio pulsars in compact trajectories around Sagittarius A* would permit an unprecedented and detailed investigation of the relativistic space–time of this supermassive black hole. Once a pulsar is detected in a compact trajectory around Sagittarius A*, continuous timing will allow more measurements and tests as the timing baseline grows with time. After timing one trajectory, all Kepplerian parameters will be well known and also the post–Kepplerian perenigricon advance will be measured with high precision. This will already provide a good estimate of the mass m_0 of Sagittarius A*. Timing a few more of the trajectories would then allow the determination of additional post–Kepplerian parameters. These parameters permit a robust determination of Sagittarius A* mass and the inclination of the pulsar trajectory with respect to the line of sight ([3], [8], [23], [24], [26]).

From the mathematical point of view it is highly instructive to see how the Poincaré models of conformal non–Euclidean metrical geometry of strictly negative curvature fit projectively to the affine coadjoint orbit model $\mathrm{Lie}(\mathcal{N})^*/\mathrm{CoAd}(\mathcal{N})$ of quantum entanglement in the ambient conformally projectivized dual vector space $\mathrm{PLie}(\mathcal{N})^*$ associated with the three–dimensional real Heisenberg Lie group $\mathcal{N} \cong \mathbb{C}_{\mathbb{R}} \oplus \mathbb{R}$. As opposed to the tesselations of hyperbolic geometry, there exists only a finite number of tilings in the Euclidean and elliptic geometries ([2]).

References

[1] J.C. Baez, The octonions. Bull. (New Series) Amer. Math. Soc. 39, 145–205 (2002)

[2] A.F. Beardon, The Geometry of Discrete Groups. Springer–Verlag, New York, Heidelberg, Berlin 1983

[3] W. Becker, Editor, Neutron Stars and Pulsars. Springer–Verlag, Berlin, Heidelberg, New York 2009

[4] D.E. Blair, Inversion Theory and Conformal Mapping. Amer. Math. Soc., Providence, Rhode Island 2000

[5] W.R. Brown, M. Kilic, J.J. Hermes, C.A. Prieto, S.J. Kenyon, D.E. Winget, A 12 minute orbital period detached white dwarf eclipsing binary. The Astrophys. J. Lett. 737: L23, 1–6 (2011)

[6] B. Cordani, The Kepler Problem: Group Theoretical Aspects, Regularization and Quantization, with Applications to the Study of Perturbations. Birkhäuser Verlag, Basel, Boston, Berlin 2003

[7] D. M. Dubois, Incursive Algorithms for Newtonian and Relativistic Gravitations, and Simulation of the Mercury Orbit. International Journal of Computing Anticipatory Systems, Vol. 20, pp. 3–16 (2008) ISSN 1373-5411

[8] F. Eisenhauer, R. Schödel, R. Genzel, T. Ott, M. Tecza, R. Abuter, A. Eckart, T. Alexander, A geometric determination of the distance to the galactic center. The Astrophys. J. 597, L121–L124 (2003)

[9] G.F.R. Ellis, R. Maartens, M.A.H. MacCallum, Relativistic Cosmology. Cambridge University Press, Cambridge, New York, Melbourne 2012

[10] H. Falcke, F. Melia, E. Agol, Viewing the shadow of the black hole at the galactic center. The Astroph. J. Lett. 528, L13–L16 (2000)

[11] R. Genzel, F. Eisenhauer, S. Gillessen, The Galactic Center massive black hole and nuclear star cluster. Rev. Mod. Phys. 82, 3121–3195 (2010)

[12] A.M. Ghez, S. Salim, S.D. Hornstein, A. Tanner, J.R. Lu, M. Morris, E.E. Becklin, G. Duchêne, Stellar orbits around the galactic center black hole. The Astrophys. J. 620, 744–757 (2005)

[13] S. Gillessen, F. Eisenhauer, S. Trippe, T. Alexander, R. Genzel, F. Martins, T. Ott, Monitoring stellar orbits around the massive black hole in the galactic center. The Astrophys. J. 692, 1075–1109 (2009)

[14] A. Guichardet, Théorie de Mackey et méthode des orbites selon M. Duflo. Expo. Math. 3, 303–346 (1985)

[15] F. Guillod, P. Huguenin, Canonical scattering transformation in quantum mechanics. J. Phys. A: Math. Gen. 15, 3705–3714 (1982)

[16] R.O. Hansen, Multipole moments of stationary space–times. J. Math. Phys. 15, 46–52 (1974)

[17] S.W. Hawking, G.F.R. Ellis, The Large Scale Structure of Space–Time. Cambridge University Press, Cambridge, New York, Melbourne 1973

[18] S.W. Hawking, W. Israel, Editors, General Relativity: an Einstein Centenary Survey. Two volumes, Cambridge University Press, Cambridge, New York, Melbourne 2010

[19] F. Hirzebruch, Topological Methods in Algebraic Geometry. Third Enlarged Edition, Springer–Verlag, Berlin, Heidelberg, New York 1966

[20] B. Kostant, Quantization and unitary representations. In: Lectures in Modern Analysis and Applications III, C.T. Taam, Editor, pp. 87–208, Lecture Notes in Math., Vol. 170, Springer–Verlag, Berlin, Heidelberg, New York 1970

[21] B. Kostant, Symplectic spinors. Symposia Mathematica, Vol. XIV, pp. 139–152, Academic Press, London, New York 1974

[22] P.D. Lax, R.S. Phillips, Scattering Theory of Automorphic Functions. Annals of Mathematics Studies 87, Priceton University Press, Princeton, New Jersey 1976

[23] K. Liu, N. Wex, M. Kramer, J.M. Cordes, T.J.W. Lazio, Prospects for probing the spacetime of Sgr A* with pulsars. The Astrophys. J. 747, 1–11 (2012)

[24] D.R. Lorimer, M. Kramer, Handbook of Pulsar Astronomy. Cambridge University Press, Cambridge, New York, Melbourne 2005

[25] J.R. Lu, A.M. Ghez, S.D. Hornstein, M. Morris, K. Matthews, D.J. Thompson, E.E. Becklin, Galactic center youth: Orbits and origins of the young stars in the central parsec. J. Phys.: Conf. Ser. 54, 279–287 (2006)

[26] A.G. Lyne, F. Graham–Smith, Pulsar Astronomy. Third edition, Cambridge University Press, Cambridge, New York, Melbourne 2005

[27] F. Melia, The Black Hole at the Center of Our Galaxy. Princeton University Press, Princeton, New Jersey 2003

[28] D.J. Nice, R.W. Sayer, J.H. Taylor, PSR J1518+4904: A mildly relativistic binary pulsar system. The Astrophys. J. 466, L87–L90 (1996)

[29] R. Penrose, W. Rindler, Spinors and Space–Time. Two Volumes, Cambridge University Press, Cambridge, New York, Melbourne 2008

[30] R.K. Sachs, H.–H. Wu, General Relativity for Mathematicians. Springer–Verlag, New York, Heidelberg, Berlin 1977

[31] W.J. Schempp, Magnetic Resonance Imaging: Mathematical Foundations and Applications. Wiley–Liss, New York, Chichester, Weinheim 1998

[32] W.J. Schempp, The conformal steady state free precession: A Kepplerian approach to automorphic scattering theory of orbiton/spinon dynamics. Proceedings of the Vigier VIII Symposium - BCS Joint Meeting, World Scientific Publishing, Singapore 2013

[33] R. Schödel, R. Genzel, T. Ott, A star in a 15.2–year orbit around the supermassive black hole at the centre of the Milky Way. Nature 419, 694–696 (2002)

[34] R. Schödel, Sagittarius A* in the Infrared. J. Phys.: Conf. Ser. 372, 012020–1 to 012020–6 (2012)

[35] D.J. Simms, Geometric quantization of energy levels in the Kepler problem. In: Symposia Mathematica, Vol. XIV, pp. 125–137, Academic Press, London, New York 1974

[36] J.–M. Souriau, Sur la variété de Képler. Symposia Mathematica, Vol. XIV, pp. 343–360, Academic Press, London, New York 1974

[37] J.–M. Souriau, Structure of Dynamical Systems: A Symplectic View of Physics. Birkhäuser Verlag, Basel, Boston, Berlin 1997

[38] B. Stephenson, Kepler's Physical Astronomy. Princeton University Press, Princeton, New Jersey 1994

[39] E.L. Stiefel, G. Scheifele, Linear and Regular Celestial Mechanics. Springer–Verlag, Berlin, Heidelberg, New York 1971

[40] J.H. Taylor, Pulsar timing and relativistic gravity. Class. Quantum Grav. 10, S167–S174 (1993)

[41] J.H. Taylor, R.A. Hulse, L.A. Fowler, G.E. Gullahorn, J.M. Rankin, Further observations of the binary pulsar PSR 1913+16. The Astrophys. J. 206, L53–L58 (1976)

[42] R.C.E. van den Bosch, K. Gebhardt, K. Gültekin, G. van de Ven, A. van der Wel, J.L. Walsh, An over–massive black hole in the compact lenticular galaxy NGC 1277. Nature 491, 729–731 (2012)

[43] A. Weil, Introduction à l'Étude des Variétés Kählériennes. Hermann, Paris 1958

[44] A. Weil, Sur certains groupes d'opérateurs unitaires. Acta Math. 111, 143–211 (1964); Collected Papers, Vol. III, pp. 1–69, Springer–Verlag, New York, Heidelberg, Berlin 1979

[45] J.M. Weisberg, D.J. Nice, J.H. Taylor, Timing measurement of the relativistic binary pulsar PSR B1913+16. The Astrophys. J. 722, 1030–1034 (2010)

[46] D.L. Wiltshire, M. Visser, S.M. Scott, Editors, The Kerr Spacetime: Rotating Black Holes in General Relativity. Cambridge University Press, Cambridge, New York, Melbourne 2009